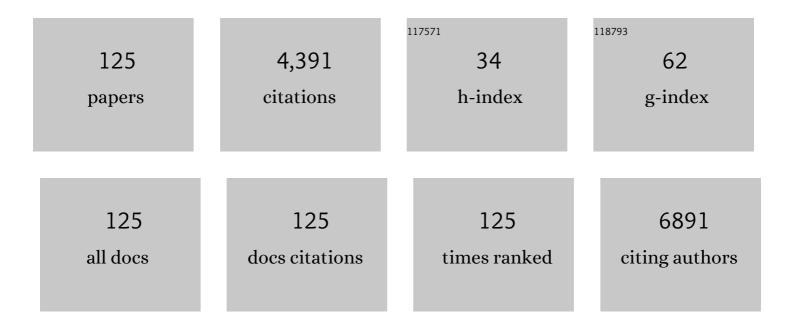
List of Publications by Year in descending order

Source: https://exaly.com/author-pdf/7018670/publications.pdf Version: 2024-02-01



Οτα Ερανικ

#	Article	IF	CITATIONS
1	Influence of structural properties on (de-)intercalation of ClO4â^' anion in graphite from concentrated aqueous electrolyte. Carbon, 2022, 186, 612-623.	5.4	10
2	Probing the local dielectric function of WS2 on an Au substrate by near field optical microscopy operating in the visible spectral range. Applied Surface Science, 2022, 574, 151672.	3.1	6
3	Chaotropic anion based "water-in-salt―electrolyte realizes a high voltage Zn–graphite dual-ion battery. Journal of Materials Chemistry A, 2022, 10, 2064-2074.	5.2	28
4	Reversible anion intercalation into graphite from aluminum perchlorate "waterâ€inâ€saltâ€electrolyte. Electrochimica Acta, 2022, 404, 139754.	2.6	9
5	Localized Spectroelectrochemical Identification of Basal Plane and Defect-Related Charge-Transfer Processes in Graphene. Journal of Physical Chemistry Letters, 2022, 13, 642-648.	2.1	8
6	Approach to map nanotopography of cell surface receptors. Communications Biology, 2022, 5, 218.	2.0	6
7	Activation of Raman modes in monolayer transition metal dichalcogenides through strong interaction with gold. Physical Review B, 2022, 105, .	1.1	9
8	Nano-optical Visualization of Interlayer Interactions in WSe ₂ /WS ₂ Heterostructures. Journal of Physical Chemistry Letters, 2022, 13, 5854-5859.	2.1	5
9	Evolution of the Raman 2D' mode in monolayer graphene during electrochemical doping. Microchemical Journal, 2022, 181, 107739.	2.3	3
10	Wrinkle development in graphene sheets with patterned nano-protrusions: A molecular dynamics study. Carbon, 2021, 173, 301-310.	5.4	6
11	Chemical vapor deposition (CVD) growth of graphene films. , 2021, , 199-222.		4
12	Strong localization effects in the photoluminescence of transition metal dichalcogenide heterobilayers. 2D Materials, 2021, 8, 025028.	2.0	19
13	Direct visualization of local deformations in suspended few-layer graphene membranes by coupled in situ atomic force and scanning electron microscopy. Applied Physics Letters, 2021, 118, 103104.	1.5	3
14	In Situ Raman Microdroplet Spectroelectrochemical Investigation of CuSCN Electrodeposited on Different Substrates. Nanomaterials, 2021, 11, 1256.	1.9	3
15	Superradiant Emission from Coherent Excitons in van Der Waals Heterostructures. Advanced Functional Materials, 2021, 31, 2102196.	7.8	12
16	Two-Dimensional CVD-Graphene/Polyaniline Supercapacitors: Synthesis Strategy and Electrochemical Operation. ACS Applied Materials & Interfaces, 2021, 13, 34686-34695.	4.0	30
17	Electron-phonon coupling origin of the graphene ï€* -band kink via isotope effect. Physical Review B, 2021, 103, .	1.1	3
18	Biaxial strain engineering of CVD and exfoliated single- and bi-layer MoS ₂ crystals. 2D Materials, 2021, 8, 015023.	2.0	26

#	Article	IF	CITATIONS
19	Hierarchy of nanoscale graphene wrinkles on compliant substrate: Theory and experiment. Extreme Mechanics Letters, 2020, 40, 100948.	2.0	2
20	The Intricate Love Affairs between MoS ₂ and Metallic Substrates. Advanced Materials Interfaces, 2020, 7, 2001324.	1.9	15
21	Rippled Metallicâ€Nanowire/Graphene/Semiconductor Nanostack for a Gateâ€Tunable Ultrahighâ€Performance Stretchable Phototransistor. Advanced Optical Materials, 2020, 8, 2000859.	3.6	5
22	Periodic surface functional group density on graphene via laser-induced substrate patterning at Si/SiO2 interface. Nano Research, 2020, 13, 2332-2339.	5.8	14
23	Chemical Vapor Deposition of MoS ₂ for Energy Harvesting: Evolution of the Interfacial Oxide Layer. ACS Applied Nano Materials, 2020, 3, 6563-6573.	2.4	10
24	Strain and Charge Doping Fingerprints of the Strong Interaction between Monolayer MoS ₂ and Gold. Journal of Physical Chemistry Letters, 2020, 11, 6112-6118.	2.1	77
25	Transferless Inverted Graphene/Silicon Heterostructures Prepared by Plasma-Enhanced Chemical Vapor Deposition of Amorphous Silicon on CVD Graphene. Nanomaterials, 2020, 10, 589.	1.9	3
26	IMPOSING BIAXIAL STRAIN ON 2D LAYERED MATERIALS BY LIQUID-INDUCED SWELLING OF SUPPORTING POLYMER. , 2020, , .		0
27	Rutile TiO2 thin film electrodes with excellent blocking function and optical transparency. Electrochimica Acta, 2019, 321, 134685.	2.6	19
28	On the Suitability of Raman Spectroscopy to Monitor the Degree of Graphene Functionalization by Diazonium Salts. Journal of Physical Chemistry C, 2019, 123, 22397-22402.	1.5	14
29	Superlattice in collapsed graphene wrinkles. Scientific Reports, 2019, 9, 9972.	1.6	15
30	lmaging Nanoscale Inhomogeneities and Edge Delamination in Asâ€Grown MoS ₂ Using Tipâ€Enhanced Photoluminescence. Physica Status Solidi - Rapid Research Letters, 2019, 13, 1900381.	1.2	12
31	Determination of atomic boron concentration in heavily boron-doped diamond by Raman spectroscopy. Diamond and Related Materials, 2019, 93, 54-58.	1.8	47
32	Sculpturing graphene wrinkle patterns into compliant substrates. Carbon, 2019, 146, 772-778.	5.4	18
33	Strong and efficient doping of monolayer MoS ₂ by a graphene electrode. Physical Chemistry Chemical Physics, 2019, 21, 25700-25706.	1.3	20
34	Evaluating arbitrary strain configurations and doping in graphene with Raman spectroscopy. 2D Materials, 2018, 5, 015016.	2.0	95
35	Local Photovoltaic Properties of Graphene–Silicon Heterojunctions (Phys. Status Solidi B 12/2018). Physica Status Solidi (B): Basic Research, 2018, 255, 1870144.	0.7	0
36	Local Photovoltaic Properties of Graphene–Silicon Heterojunctions. Physica Status Solidi (B): Basic Research, 2018, 255, 1800305.	0.7	4

#	Article	IF	CITATIONS
37	Electrochemical characterization of porous boron-doped diamond prepared using SiO2 fiber template. Diamond and Related Materials, 2018, 87, 61-69.	1.8	36
38	Analysis of heavily boron-doped diamond Raman spectrum. Diamond and Related Materials, 2018, 88, 163-166.	1.8	52
39	Insight into boron-doped diamond Raman spectra characteristic features. Carbon, 2017, 115, 279-284.	5.4	103
40	Fine tuning of optical transition energy of twisted bilayer graphene via interlayer distance modulation. Physical Review B, 2017, 95, .	1.1	12
41	Optically transparent composite diamond/Ti electrodes. Carbon, 2017, 119, 179-189.	5.4	18
42	Temperature-induced strain release via rugae on the nanometer and micrometer scale in graphene monolayer. Carbon, 2017, 119, 483-491.	5.4	13
43	SERS of Isotopically Labeled ¹² C/ ¹³ C Graphene Bilayer–Gold Nanostructured Film Hybrids: Graphene Layer as Spacer and SERS Probe. Journal of Physical Chemistry C, 2017, 121, 11680-11686.	1.5	8
44	Tuning the electronic properties of monolayer and bilayer transition metal dichalcogenide compounds under direct out-of-plane compression. Physical Chemistry Chemical Physics, 2017, 19, 13333-13340.	1.3	20
45	Photovoltaic characterization of graphene/silicon Schottky junctions from local and macroscopic perspectives. Chemical Physics Letters, 2017, 676, 82-88.	1.2	9
46	Fabrication of porous boron-doped diamond on SiO2 fiber templates. Carbon, 2017, 114, 457-464.	5.4	68
47	Mastering the Wrinkling of Self-supported Graphene. Scientific Reports, 2017, 7, 10003.	1.6	33
48	Tuning the Interlayer Interaction of a Twisted Multilayer Wrinkle With Temperature. Physica Status Solidi (B): Basic Research, 2017, 254, 1700237.	0.7	2
49	Wrinkled Few-Layer Graphene as Highly Efficient Load Bearer. ACS Applied Materials & Interfaces, 2017, 9, 26593-26601.	4.0	46
50	High pressure Raman studies of single- and bi-layer graphene on copper. Journal of Physics: Conference Series, 2017, 950, 032006.	0.3	1
51	In situ Raman spectroelectrochemistry as a useful tool for detection of TiO2(anatase) impurities in TiO2(B) and TiO2(rutile). Monatshefte Für Chemie, 2016, 147, 951-959.	0.9	24
52	n-Type phosphorus-doped nanocrystalline diamond: electrochemical and in situ Raman spectroelectrochemical study. RSC Advances, 2016, 6, 51387-51393.	1.7	12
53	Addressing Raman features of individual layers in isotopically labeled Bernal stacked bilayer graphene. 2D Materials, 2016, 3, 025022.	2.0	8
54	Structural, optical and mechanical properties of thin diamond and silicon carbide layers grown by low pressure microwave linear antenna plasma enhanced chemical vapour deposition. Diamond and Related Materials, 2016, 69, 13-18.	1.8	20

#	Article	IF	CITATIONS
55	The pink pigment prodigiosin: Vibrational spectroscopy and DFT calculations. Dyes and Pigments, 2016, 134, 234-243.	2.0	9
56	Do defects enhance fluorination of graphene?. RSC Advances, 2016, 6, 81471-81476.	1.7	10
57	Graphene under direct compression: Stress effects and interlayer coupling. Physica Status Solidi (B): Basic Research, 2016, 253, 2336-2341.	0.7	7
58	Monitoring the doping of graphene on SiO ₂ /Si substrates during the thermal annealing process. RSC Advances, 2016, 6, 72859-72864.	1.7	24
59	Temperature dependence of the 2D′ mode of an isotopically labelled graphene double layer. Physica Status Solidi (B): Basic Research, 2016, 253, 2342-2346.	0.7	0
60	Stress and charge transfer in uniaxially strained CVD graphene. Physica Status Solidi (B): Basic Research, 2016, 253, 2355-2361.	0.7	12
61	Addressing asymmetry of the charge and strain in a two-dimensional fullerene peapod. Nanoscale, 2016, 8, 735-740.	2.8	6
62	Effect of layer number and layer stacking registry on the formation and quantification of defects in graphene. Carbon, 2016, 98, 592-598.	5.4	16
63	Graphene wrinkling induced by monodisperse nanoparticles: facile control and quantification. Scientific Reports, 2015, 5, 15061.	1.6	35
64	Fluorination of Isotopically Labeled Turbostratic and Bernal Stacked Bilayer Graphene. Chemistry - A European Journal, 2015, 21, 1081-1087.	1.7	25
65	Raman Spectroscopy and <i>in Situ</i> Raman Spectroelectrochemistry of Isotopically Engineered Graphene Systems. Accounts of Chemical Research, 2015, 48, 111-118.	7.6	55
66	Temperature and face dependent copper–graphene interactions. Carbon, 2015, 93, 793-799.	5.4	24
67	Boron-doped Diamond Electrodes: Electrochemical, Atomic Force Microscopy and Raman Study towards Corrosion-modifications at Nanoscale. Electrochimica Acta, 2015, 179, 626-636.	2.6	35
68	Graphene Mechanics: Current Status and Perspectives. Annual Review of Chemical and Biomolecular Engineering, 2015, 6, 121-140.	3.3	76
69	Single Layer Molybdenum Disulfide under Direct Out-of-Plane Compression: Low-Stress Band-Gap Engineering. Nano Letters, 2015, 15, 3139-3146.	4.5	75
70	Electrochemical impedance spectroscopy of polycrystalline boron doped diamond layers with hydrogen and oxygen terminated surface. Diamond and Related Materials, 2015, 55, 70-76.	1.8	26
71	Water as a Promoter and Catalyst for Dioxygen Electrochemistry in Aqueous and Organic Media. ACS Catalysis, 2015, 5, 6600-6607.	5.5	98
72	Strain Assessment in Graphene Through the Raman 2D′ Mode. Journal of Physical Chemistry C, 2015, 119, 25651-25656.	1.5	38

#	Article	IF	CITATIONS
73	Preparation and Charge-Transfer Study in a Single-Walled Carbon Nanotube Functionalized with Poly(3,4-ethylenedioxythiophene). Journal of Physical Chemistry C, 2015, 119, 21538-21546.	1.5	11
74	Thermal treatment of fluorinated graphene: An in situ Raman spectroscopy study. Carbon, 2015, 84, 347-354.	5.4	27
75	High-quality graphene on single crystal Ir(1 1 1) films on Si(1 1 1) wafers: Synthesis and multi-spectroscopic characterization. Carbon, 2015, 81, 167-173.	5.4	11
76	Interaction of Human Osteoblast-Like Saos-2 and MG-63 Cells with Thermally Oxidized Surfaces of a Titanium-Niobium Alloy. PLoS ONE, 2014, 9, e100475.	1.1	47
77	Progressive In Situ Reduction of Graphene Oxide Studied by Raman Spectroelectrochemistry: Implications for a Spontaneous Activation of LiFePO ₄ (Olivine). Electroanalysis, 2014, 26, 57-61.	1.5	8
78	Interaction between graphene and copper substrate: The role of lattice orientation. Carbon, 2014, 68, 440-451.	5.4	180
79	Chemical vapor deposition (CVD) growth of graphene films. , 2014, , 27-49.		11
80	Carbon isotope labelling in graphene research. Nanoscale, 2014, 6, 6363.	2.8	38
81	Heating Isotopically Labeled Bernal Stacked Graphene: A Raman Spectroscopy Study. Journal of Physical Chemistry Letters, 2014, 5, 549-554.	2.1	33
82	Growth of adlayers studied by fluorination of isotopically engineered graphene. Physica Status Solidi (B): Basic Research, 2014, 251, 2505-2508.	0.7	5
83	Failure Processes in Embedded Monolayer Graphene under Axial Compression. Scientific Reports, 2014, 4, 5271.	1.6	65
84	Raman spectroscopy of graphene at high pressure: Effects of the substrate and the pressure transmitting media. Physical Review B, 2013, 88, .	1.1	56
85	Lithium Insertion into Titanium Dioxide (Anatase): A Raman Study with ^{16/18} O and ^{6/7} Li Isotope Labeling. Chemistry of Materials, 2013, 25, 3710-3717.	3.2	17
86	On the role of Nb-related sites of an oxidized β-TiNb alloy surface in its interaction with osteoblast-like MG-63 cells. Materials Science and Engineering C, 2013, 33, 1636-1645.	3.8	63
87	Conductivity of boron-doped polycrystalline diamond films: influence of specific boron defects. European Physical Journal B, 2013, 86, 1.	0.6	55
88	Electrochemistry and in situ Raman spectroelectrochemistry of low and high quality boron doped diamond layers in aqueous electrolyte solution. Electrochimica Acta, 2013, 87, 518-525.	2.6	65
89	Raman spectroscopy investigation of defect occurrence in graphene grown on copper single crystals. Physica Status Solidi (B): Basic Research, 2013, 250, 2653-2658.	0.7	7
90	Mass-related inversion symmetry breaking and phonon self-energy renormalization in isotopically labeled AB-stacked bilayer graphene. Scientific Reports, 2013, 3, 2061.	1.6	17

#	Article Isologyic <mml:math.xmlns:mml="http: 1998="" math="" mathml"<="" th="" www.w3.org=""><th>IF</th><th>CITATIONS</th></mml:math.xmlns:mml="http:>	IF	CITATIONS
91	display="inline"> <mml:msup><mml:mrow /><mml:mn>13</mml:mn></mml:mrow </mml:msup> C/ <mml:math xmlns:mml="http://www.w3.org/1998/Math/MathML" display="inline"><mml:msup><mml:mrow /><mml:mn>12</mml:mn></mml:mrow </mml:msup>C effect on the resonant Raman spectrum of twisted</mml:math 	1.1	13
92	bilayer graphene. Physical Review B, 2013, 88, . In situ Raman spectroelectrochemistry of graphene oxide. Physica Status Solidi (B): Basic Research, 2013, 250, 2662-2667.	0.7	26
93	Effects of Heat Treatment on Raman Spectra of Two‣ayer ¹² C/ ¹³ C Graphene. Chemistry - A European Journal, 2012, 18, 13877-13884.	1.7	34
94	Raman spectra of titanium dioxide (anatase, rutile) with identified oxygen isotopes (16, 17, 18). Physical Chemistry Chemical Physics, 2012, 14, 14567.	1.3	417
95	Phonon and Structural Changes in Deformed Bernal Stacked Bilayer Graphene. Nano Letters, 2012, 12, 687-693.	4.5	65
96	Large Variations of the Raman Signal in the Spectra of Twisted Bilayer Graphene on a BN Substrate. Journal of Physical Chemistry Letters, 2012, 3, 796-799.	2.1	30
97	The control of graphene double-layer formation in copper-catalyzed chemical vapor deposition. Carbon, 2012, 50, 3682-3687.	5.4	120
98	Axial Deformation of Monolayer Graphene under Tension and Compression. Carbon Nanostructures, 2012, , 87-97.	0.1	2
99	Raman 2D-Band Splitting in Graphene: Theory and Experiment. ACS Nano, 2011, 5, 2231-2239.	7.3	271
100	Development of a universal stress sensor for graphene and carbon fibres. Nature Communications, 2011, 2, .	5.8	172
101	Surface refinement and electronic properties of graphene layers grown on copper substrate: An XPS, UPS and EELS study. Applied Surface Science, 2011, 257, 9785-9790.	3.1	185
102	Nanobubble-assisted formation of carbon nanostructures on basal plane highly ordered pyrolytic graphite exposed to aqueous media. Nanotechnology, 2010, 21, 095707.	1.3	29
103	Compression Behavior of Single-Layer Graphenes. ACS Nano, 2010, 4, 3131-3138.	7.3	282
104	Carbon Nanotube Electrodes for Hotâ€Wire Electrochemistry. ChemPhysChem, 2009, 10, 559-563.	1.0	13
105	Photoluminescence of nanoporous silicon grains in TiO ₂ matrices. Physica Status Solidi C: Current Topics in Solid State Physics, 2009, 6, 1713-1716.	0.8	1
106	Supramolecular Assembly of Single-Walled Carbon Nanotubes with a Ruthenium(II)â^Bipyridine Complex: An in Situ Raman Spectroelectrochemical Study. Journal of Physical Chemistry C, 2009, 113, 2611-2617.	1.5	8
107	Optimizing Conditions for Ultrasound Extraction of Fullerenes from Coal Matrices. Fullerenes Nanotubes and Carbon Nanostructures, 2009, 17, 109-122.	1.0	10
108	Novel Synthesis of the TiO2(B) Multilayer Templated Films. Chemistry of Materials, 2009, 21, 1457-1464.	3.2	69

#	Article	IF	CITATIONS
109	Self-Assemblies of Cationic Porphyrins with Functionalized Water-Soluble Single-Walled Carbon Nanotubes. Journal of Nanoscience and Nanotechnology, 2009, 9, 5795-5802.	0.9	8
110	Inâ€situ Vis/NIR spectroelectrochemistry of singleâ€walled carbon nanotubes enriched with (6,5) tubes. Physica Status Solidi (B): Basic Research, 2008, 245, 2239-2242.	0.7	7
111	In Situ Raman Spectroelectrochemistry of Single-Walled Carbon Nanotubes: Investigation of Materials Enriched with (6,5) Tubes. Journal of Physical Chemistry C, 2008, 112, 14179-14187.	1.5	22
112	Multilayer Films from Templated TiO ₂ and Structural Changes during their Thermal Treatment. Chemistry of Materials, 2008, 20, 2985-2993.	3.2	59
113	Heterostructures from Single-Wall Carbon Nanotubes and TiO[sub 2] Nanocrystals. Journal of the Electrochemical Society, 2007, 154, K19.	1.3	15
114	Raman spectroscopy as tool for the characterization of thio-polyaromatic hydrocarbons in organic minerals. Spectrochimica Acta - Part A: Molecular and Biomolecular Spectroscopy, 2007, 68, 1065-1069.	2.0	28
115	Structural properties and electrochemical behavior of CNTâ€TiO ₂ nanocrystal heterostructures. Physica Status Solidi (B): Basic Research, 2007, 244, 4040-4045.	0.7	17
116	Raman spectroscopic study of the complex aromatic mineral idrialite. Journal of Raman Spectroscopy, 2006, 37, 771-776.	1.2	24
117	Fullerene C60 in Solid Bitumen Accumulations in Neo-Proterozoic Pillow-Lavas at MÃŧov (Bohemian) Tj ETQq1 1	0.784314	rgBT /Overic
118	Fullerene Synthesis by Alteration of Coal and Shale by Simulated Lightning. , 2006, , 241-255.		1
119	Evaluation of Raman spectroscopy to detect fullerenes in geological materials. Spectrochimica Acta - Part A: Molecular and Biomolecular Spectroscopy, 2005, 61, 2364-2367.	2.0	10
120	Low extraction recovery of fullerene from carbonaceous geological materials spiked with C60. Carbon, 2005, 43, 1909-1917.	5.4	37
121	The search for fullerenes in rocks from the Ries impact crater. Meteoritics and Planetary Science, 2005, 40, 307-314.	0.7	3
122	Amino acid formation induced by high-power laser in CO2/CO–N2–H2O gas mixtures. Chemical Physics Letters, 2004, 386, 169-173.	1.2	41
123	Evidence for fullerenes in solid bitumen from pillow lavas of Proterozoic age from MÃŧov (Bohemian) Tj ETQq1 1	0.784314 1.6	rg <u>B</u> T /Overlo
124	Search for Fullerenes in Geological Carbonaceous Samples Altered by Experimental Lightning. Fullerenes Nanotubes and Carbon Nanostructures, 2003, 11, 257-267.	1.0	2
125	Electrochromic 2,5â€Dihydroxyterephthalic Acid Linker in Metalâ^'Organic Frameworks. Advanced Photonics Research, 0, , 2100219.	1.7	1